arXiv:1404.5833v2 [cond-mat.mes-hall] 24 Apr 2014

Atomic monolayer deposition on the surface of nanotube mechanical resonators

A. Tavernarakis,[1] J. Chaste,[2,*] A. Eichler,[1,2,†] G. Ceballos,[2] M. C. Gordillo,[3] J. Boronat,[4] and A. Bachtold[1,2]

[1]*ICFO - Institut de Ciencies Fotoniques, Mediterranean Technology Park, 08860 Castelldefels, Barcelona, Spain*

[2]*Institut Català de Nanotecnologia, Campus de la UAB, E-08193 Bellaterra, Spain*

[3]*Departamento de Sistemas Físicos, Químicos y Naturales, Universidad Pablo de Olavide, Carretera de Utrera, km 1, E-41013 Sevilla, Spain*

[4]*Departament de Física i Enginyeria Nuclear, Universitat Politècnica de Catalunya, B4-B5 Campus Nord, 08034 Barcelona, Spain*

Abstract

We studied monolayers of noble gas atoms (Xe, Kr, Ar, and Ne) deposited on individual ultra-clean suspended nanotubes. For this, we recorded the resonance frequency of the mechanical motion of the nanotube, since it provides a direct measure of the coverage. The latter is the number of adsorbed atoms divided by the number of the carbon atoms of the suspended nanotube. Monolayers formed when the temperature was lowered in a constant pressure of noble gas atoms. The coverage of Xe monolayers remained constant at 1/6 over a large temperature range. This finding reveals that Xe monolayers are solid phases with a triangular atomic arrangement, and are commensurate with the underlying carbon nanotube. By comparing our measurements to theoretical calculations, we identify the phases of Ar and Ne monolayers as fluids, and we tentatively describe Kr monolayers as solid phases. These results underscore that mechanical resonators made from single nanotubes are excellent probes for surface science.

PACS numbers: 68.43.-h, 62.25.Jk, 81.07.De

Keywords:

Carbon nanotubes have motivated a considerable research effort for the study of gas adsorption onto substrates that approach the one-dimensional limit [1–9]. Many studies have been carried out on mats and films of nanotube bundles, but the interpretation of those measurements is complicated by the fact that the binding energy of the gas atoms on the substrate is not homogeneous. That is, the binding energy depends on whether the atom is located on an individual nanotube, at the junction between two crossing nanotubes, or along the interstitial channel formed between two parallel nanotubes. Recently, this homogeneity problem was solved by studying gas adsorption on individual nanotubes, a technical feat considering the tiny amount of adsorbed atoms [7–9]. For this, nanotubes were employed both as substrates for adsorption and as detectors. Namely, the nanotubes were operated as mechanical resonators, the resonance frequency being exquisitely sensitive to the number of adsorbed atoms [9–12].

Atoms adsorbed on graphitic surfaces can form a rich variety of different phases, such as vapor, liquid, supercritical fluids, and solids [13]. The solid phase can be either commensurate or incommensurate with the graphene surface (Fig. 1(a,b)). The commensurate solid phase is robust, since the crystal formed by the adsorbed atoms is strongly pinned to the underlying carbon surface. Commensurate monolayers on graphite feature a well defined ratio between the number of adsorbed atoms and the number of carbon atoms at the surface. This ratio, called coverage, is often 1/6 for noble gas atoms, which corresponds to a registered $\sqrt{3} \times \sqrt{3}$ lattice (table 6.1 in Ref. [13]). This particular coverage value arises because, in this solid phase, noble gas atoms form a two-dimensional triangular arrangement in which atoms occupy the center of carbon hexagons, leaving an empty one in the center of the triangle (see Fig. 1b). Nanotubes are also expected to host commensurate solids; however, due to cylindrical boundary conditions, these solids exist only for some specific nanotube chiralities (n, m), namely when $(n - m)/3$ is an integer [7]. Remarkably, this is also the condition for nanotubes to be metallic.

Solid and fluid monolayers made of noble gas atoms, such as Xe, Kr, and Ar, were measured on graphite surfaces only when the coverage was comparable to or larger than 1/6 (chapter 6 in Ref. [13]). When adsorbed on a nanotube surface, the coverage of incommensurate solids and fluids is expected to become larger than that measured on graphite due to the curvature of the nanotube [8]. This is because (i) adsorbed atoms form cylindrical monolayers with a surface larger than that of the carbon nanotube, and (ii) the two-dimensional

density of noble gas atoms is, to a good approximation, independent of the curvature of the monolayer. Recently, monolayers of Kr and Ar were obtained on individual nanotubes by increasing the pressure of Kr or Ar gas surrounding the nanotube [7]. These monolayers were identified as solids, but these phases were fragile, since the number of atoms in the monolayer was very sensitive to temperature.

Here, we report on the formation of monolayers of Xe, Kr, Ar, and Ne on individual ultra-clean nanotubes upon decreasing temperature. The pressure was kept constant, typically in the 10^{-7} mbar range. We prepared the nanotube by thoroughly current annealing it in order to remove contamination from the surface. The monolayer of Xe was found to be the most robust phase. Its coverage remained constant at 1/6 over a large temperature range, indicating the formation of a $\sqrt{3}\times\sqrt{3}$ commensurate solid. The coverages of the monolayers made from Kr, Ar, and Ne were less stable against temperature variations. We compare our experimental findings to theoretical calculations in order to establish the nature of these phases.

In order to demonstrate commensurate solid phases, we fabricated resonators based on ultra-clean nanotubes that are metallic. For this, we used the fabrication process that we described in Ref. [14]. As shown in Fig. 1(c), the nanotube is contacted by two electrodes and is suspended over a trench with a gate electrode at the bottom. The nanotube was grown by chemical vapor deposition in the last step of the fabrication process in order to reduce contamination [15] (Supplemental Material, Sec. I). The measurement of the electrical conductance as a function of the voltage applied to the gate electrode allowed us to select nanotubes that are metallic with a small energy gap (Supplemental Material, Sec. III).

The mechanical motion was driven and detected using the frequency-modulation mixing technique [16] (Supplemental Material, Sec. III). We carried out the experiment in a home-built ultra-high vacuum cryostat that reaches a base pressure of $\sim 3\cdot 10^{-11}$ mbar. The nanotube was cleaned by current annealing. Noble gas atoms were dosed from a room-temperature supply with a pinhole microdoser. We studied 3 nanotubes yielding similar results. We discuss in the following the data for one device. Data for a second device are shown in Supplementary Material, Sec. VIII.

Monolayers of noble gas atoms formed on the nanotube when the temperature (T) was lowered while keeping a constant pressure of noble gas in the cryostat chamber. The for-

mation was monitored by measuring the resonance frequency f^0 (that is, by continuously recording the response of the nanotube resonator to the driving frequency). Figure 1(d) shows prominent jumps of f^0 to lower frequencies upon lowering T (see arrows), indicating the sudden adsorption of a large quantity of atoms onto the nanotube. For comparison, when we did not dose atoms, the temperature dependence of f^0 is weak and monotonic (grey curve labeled "pristine" in Fig. 1(d)). This weak dependence is attributed to the thermal expansion of the electrodes which modifies the spring constant of the nanotube resonator [17]. The coverage at T is extracted using

$$\varphi(T) = \frac{N_{\rm ads}(T)}{N_{\rm C}} = \frac{m_{\rm C}}{m_{\rm ads}}\left[A \cdot \left(\frac{f^0_{\rm prist}(T)}{f^0_{\rm ads}(T)}\right)^2 - 1\right], \tag{1}$$

where $N_{\rm C}$ is the number of C atoms of the suspended nanotube, $N_{\rm ads}$ is the number of adsorbed atoms on the nanotube, and $m_{\rm C}$ and $m_{\rm ads}$ are the atomic masses of carbon and adsorbed atoms, respectively. Here, $f^0_{\rm ads}$ is the resonance frequency when dosing atoms for adsorption, and $f^0_{\rm prist}$ is the resonance frequency when not dosing atoms and keeping the nanotube pristine. The constant A is introduced to account for variations in the spring constant between the measurement of $f^0_{\rm ads}(T)$ and that of $f^0_{\rm prist}(T)$; indeed, the spring constant can be different, if for instance the gate voltage applied in the measurement of $f^0_{\rm ads}(T)$ differs from that of $f^0_{\rm prist}(T)$ (Supplemental Material, Sec. IV). The constant A is fixed so that $\varphi = 0$ at high T. In Eq. 1, we assume that the spring tension is insensitive to the tension induced by the interaction between noble gas atoms, which is two orders of magnitude weaker than that of covalent C-C bonds [7].

Figure 2(a) shows the temperature dependence of the coverage while dosing Kr atoms. Above a characteristic temperature $T_{\rm c} \simeq 48$ K, the coverage remains at zero. On lowering temperature, the coverage jumps to $\varphi \simeq 1/6$ and remains close to this value until $T \simeq 26$ K. This behavior can be accounted for by the balance of atoms impinging on and departing from the nanotube. For $T > T_{\rm c}$, an impinging atom departs very rapidly from the nanotube, so that the number of adsorbed atoms remains close to zero (Fig. 1(e)). For $T < T_{\rm c}$, it is energetically favourable for the atoms to stay on the nanotube (Fig. 1(f)) – the atoms forming a layer with $\varphi \simeq 1/6$. This layer is likely a monolayer, because the coverage $\varphi \simeq 1/6$ of Kr on graphite corresponds to a monolayer (chapter 6 in Ref. [13]). Upon further lowering temperature so that $T << T_{\rm c}$, the coverage gets larger than $\varphi = 1/6$, indicating that Kr atoms start to form the second layer. The coverage grows in a monotonic way

without any additional plateaus even when the coverage gets larger than one (Supplementary Material, Sec. VII). The absence of additional plateaus above $\varphi = 1/6$ further supports the interpretation of the coverage $\varphi \simeq 1/6$ as being related to the monolayer.

Key to this work is annealing the nanotube by passing a large current through it. After the measurements shown in Fig. 2(a), we exposed the nanotube to ambient air. We then baked the cryostat and the nanotube at 110 °C under vacuum for two days to reach a base pressure of $\sim 3 \cdot 10^{-11}$ mbar. We again measured the coverage upon lowering T while dosing Kr atoms. Fig. 2(b) shows that T_c is much lower than before, and the coverage at $T \lesssim T_c$ is significantly lower than 1/6. We had to anneal the nanotube with a current of ~ 10 μA in order to recover the same measurement as in Fig. 2(a). These measurements suggest that the growth of monolayers is extremely sensitive to contamination, since a simple exposure to air prevents the formation of homogeneous monolayers. Another advantage of current annealing is that it brings the nanotube back to its pristine state after the adsorption of noble gas atoms on its surface.

We grew different monolayers on the nanotube by dosing Xe, Kr, Ar, and Ne (Fig. 3). The nanotube surface was cleaned by current annealing before each growth. Upon decreasing temperature, the coverage increases rapidly from 0 to a plateau with $\varphi \simeq 1/6$, indicating the growth of the monolayer. The characteristic temperature of the monolayer growth depends on the atomic species; T_c is higher when the atomic mass is larger (Fig. 3). We attribute the origin of the variation of T_c to the polarizability of the atomic species and the van der Waals interaction between the atom and the nanotube; the polarizability and the interaction both increasing with the atomic radius. We also carried out experiments where we evaporated the monolayers from the nanotube by continuously increasing the temperature of the cryostat from 4 to ∼100 K. The coverage jumped from $\simeq 1/6$ to 0 at a temperature that is up to ∼10 K higher than T_c (Supplemental Material, Sec. V).

We measured the time of the growth of monolayers from $\varphi = 0$ to $\varphi = 1/6$ while keeping the temperature constant. This time gets longer for lower pressure (Supplementary Material, sec. VI).

Xenon monolayers are particularly robust against temperature changes. Figure 4(a) shows coverage-temperature measurements recorded at different pressures and different temperature ramping rates. T_c varies from one measurement to the next. However, the plateau in coverage at 1/6 is clearly reproducible. This shows that Xe monolayers are energetically sta-

ble with the number of atoms being insensitive to temperature over a large parameter space. In contrast, measurements with Ne feature a plateau whose coverage depends significantly on T (Fig. 4(b)).

We now discuss the nature of the monolayers of Xe, Kr, Ar, and Ne. For this, we carried out theoretical calculations to predict whether the solid phases are commensurate or incommensurate in the limit of zero temperature. In addition, we estimated the melting temperature of the different solid phases. To this end, we performed a series of Monte Carlo simulations relying on standard interatomic potentials between noble gas atoms and the carbon atoms of the nanotube (Supplementary material, Sec. IX). This microscopic study was carried out for nanotubes with diameters in the range 21–38 Å, which covers the typical diameters obtained with our chemical vapor deposition recipe.

Our experimental findings indicate that Xe monolayers are commensurate solids. Firstly, the coverage of the monolayer is 1/6. Secondly, the coverage remains at this value over a large temperature range. This robustness suggests that Xe atoms are strongly bound to the underlying carbon surface, as it is the case for commensurate solids. Our experimental results are accounted for by our theoretical calculations, which predict that the solid is a registered $\sqrt{3} \times \sqrt{3}$ crystal at zero temperature. Moreover, this solid phase is calculated to become unstable at ~ 80 K, which is consistent with the melting temperature measured in Fig. S4.

Monolayers of Ar and Ne are less stable, since the measured coverage depends significantly on temperature for $T \lesssim T_c$. Our calculations reveal that in the limit of zero temperature Ar and Ne monolayers are incommensurate solids with coverages 0.265 and 0.403, respectively. The measured coverages at $T \lesssim T_c$ are much lower than these predicted values, suggesting that the monolayers observed experimentally are not in the solid phase. Moreover, our calculations show that incommensurate solids melt at temperatures as low as 5 K when the coverage is set to the values we typically measure at $T \lesssim T_c$. This further indicates that the monolayers of Ar and Ne observed experimentally at $25 - 35$ K are in the liquid phase.

As for Kr, the measured temperature dependence of the coverage is similar to that of Xe, supporting the scenario that Kr monolayers are commensurate solid phases. This result would be in agreement with experimental signatures of stability of a commensurate Kr layer on graphite up to quite high temperatures, $T \sim 130$ K [18]. However, the coverage of Kr slightly depends on temperature in the plateau region (Fig. 3), showing that Kr

monolayers are less pinned to the carbon surface than Xe monolayers. Previous theoretical calculations of the Kr monolayer on graphite show that corrugation effects are extremely important to get the $\sqrt{3}\times\sqrt{3}$ crystal stable [19, 20]. Only by increasing in an empirical way the anisotropic part of the pair interaction the commensurate phase becomes stable. Our present simulations on Kr adsorbed on nanotubes show the same trend. Therefore, more work is needed to establish the phase of Kr monolayers on nanotubes.

To conclude, we studied the formation of noble gas atom monolayers on individual nanotubes. We found that Xe atoms form robust commensurate solids, whereas Ar and Ne atoms organize themselves in fluids. These monolayers consist of $\sim 10^5$ atoms, which is a tiny amount of material difficult to detect with most experimental techniques used in surface science. The study of these monolayers was here possible, because nanotube mechanical resonators are extremely sensitive probes. The second important aspect of our experiments is that the nanotube surface was ultra-clean; this was achieved by thoroughly current annealing the nanotube in ultra-high vacuum. These resonators made from ultra-clean nanotubes are promising for various future adsorption experiments, such as the measurement of new phase transitions emerging in the one-dimensional limit with narrower nanotubes, the investigation of quantum effects of He monolayers adsorbed on nanotubes [21], the study of the diffusion of adsorbed atoms over the resonator surface which is a topic of increasing interest [22], and the interplay between the strong mechanical nonlinearities of nanotubes [14, 23–25] and the diffusion of atoms [26–28].

We thank A. Isacsson and J. Moser for discussions. We acknowledge support from the European Union through the Graphene Flagship (604391), the ERC-carbonNEMS project, and a Marie Curie grant (271938), the Spanish state (MAT2012-31338), and the Catalan government (AGAUR, SGR). C. G. and J. B. acknowledge partial financial support from the Junta de de Andalucía Group PAI-205, Grant No. FQM-5987, MICINN (Spain) Grants No. FIS2010-18356 and FIS2011-25275, and Generalitat de Catalunya Grant 2009SGR-1003.

* Present address: CNRS, Laboratoire de Photonique et de Nanostructures, UPR20, route de Nozay, 91460 Marcoussis, France

† Present address: Department of Physics, ETH Zurich, Schafmattstrasse 16, 8093 Zurich,

Switzerland.

[1] A. Dillon, K. Jones, T. Bekkedahl, C. Kiang, D. Bethune, and M. Heben, Nature **386**, 377 (1997).

[2] W. Teizer, R. Hallock, E. Dujardin, and T. Ebbesen, Physical Review Letters **82**, 5305 (1999).

[3] H. Ulbricht, J. Kriebel, G. Moos, and T. Hertel, Chemical Physics Letters **363**, 252 (2002).

[4] W. Shi and J. K. Johnson, Physical Review Letters **91**, 015504 (2003).

[5] J.-C. Lasjaunias, K. Biljaković, J.-L. Sauvajol, and P. Monceau, Physical Review Letters **91**, 025901 (2003).

[6] H. Ulbricht, R. Zacharia, N. Cindir, and T. Hertel, Carbon **44**, 2931 (2006).

[7] Z. Wang, J. Wei, P. Morse, J. G. Dash, O. E. Vilches, and D. H. Cobden, Science **327**, 552 (2010).

[8] H.-C. Lee, O. E. Vilches, Z. Wang, E. Fredrickson, P. Morse, R. Roy, B. Dzyubenko, and D. H. Cobden, Journal of Low Temperature Physics **169**, 338 (2012).

[9] J. Chaste, A. Eichler, J. Moser, G. Ceballos, R. Rurali, and A. Bachtold, Nature Nanotechnology **7**, 301 (2012).

[10] H.-Y. Chiu, P. Hung, H. W. C. Postma, and M. Bockrath, Nano Letters **8**, 4342 (2008).

[11] B. Lassagne, D. Garcia-Sanchez, A. Aguasca, and A. Bachtold, Nano Letters **8**, 3735 (2008).

[12] K. Jensen, K. Kim, and A. Zettl, Nature Nanotechnology **3**, 533 (2008).

[13] L. W. Bruch, M. W. Cole, and E. Zaremba, Physical adsorption: forces and phenomena (Clarendon Press Oxford, 1997).

[14] A. Eichler, J. Moser, J. Chaste, M. Zdrojek, I. Wilson-Rae, and A. Bachtold, Nature Nanotechnology **6**, 339 (2011).

[15] A. K. Huttel, G. A. Steele, B. Witkamp, M. Poot, L. P. Kouwenhoven, and H. S. van der Zant, Nano Letters **9**, 2547 (2009).

[16] V. Gouttenoire, T. Barois, S. Perisanu, J.-L. Leclercq, S. T. Purcell, P. Vincent, and A. Ayari, Small **6**, 1060 (2010).

[17] J. Chaste, M. Sledzinska, M. Zdrojek, J. Moser, and A. Bachtold, Applied Physics Letters **99**, 213502 (2011).

[18] E. D. Specht, A. Mak, C. Peters, M. Sutton, R. J. Birgeneau, D. L. D'Amico, D. E. Moncton, S. E. Nagler, and P. M. Horn, Z. Phys. B **69**, 347 (1987).

[19] G. Vidali and M. W. Cole, Phys. Rev. B **29**, 6736 (1984).

[20] N. D. Shrimpton and W. A. W. A. Steele, Phys. Rev. B **44**, 3297 (1991).

[21] M. Gordillo and J. Boronat, Physical Review B **86**, 165409 (2012).

[22] Y. Yang, C. Callegari, X. Feng, and M. Roukes, Nano Letters **11**, 1753 (2011).

[23] A. Eichler, M. del Álamo Ruiz, J. Plaza, and A. Bachtold, Physical Review Letters **109**, 025503 (2012).

[24] A. Eichler, J. Moser, M. Dykman, and A. Bachtold, Nature Communications **4**, 2843 (2013).

[25] H. B. Meerwaldt, G. Labadze, B. H. Schneider, A. Taspinar, Y. M. Blanter, H. S. J. van der Zant, and G. A. Steele, Phys. Rev. B **86**, 115454 (2012).

[26] J. Atalaya, A. Isacsson, and M. Dykman, Physical Review Letters **106**, 227202 (2011).

[27] J. Atalaya, A. Isacsson, and M. I. Dykman, Phys. Rev. B **83**, 045419 (2011).

[28] A. W. Barnard, V. Sazonova, A. M. van der Zande, and P. L. McEuen, Proceedings of the National Academy of Sciences **109**, 19093 (2012).

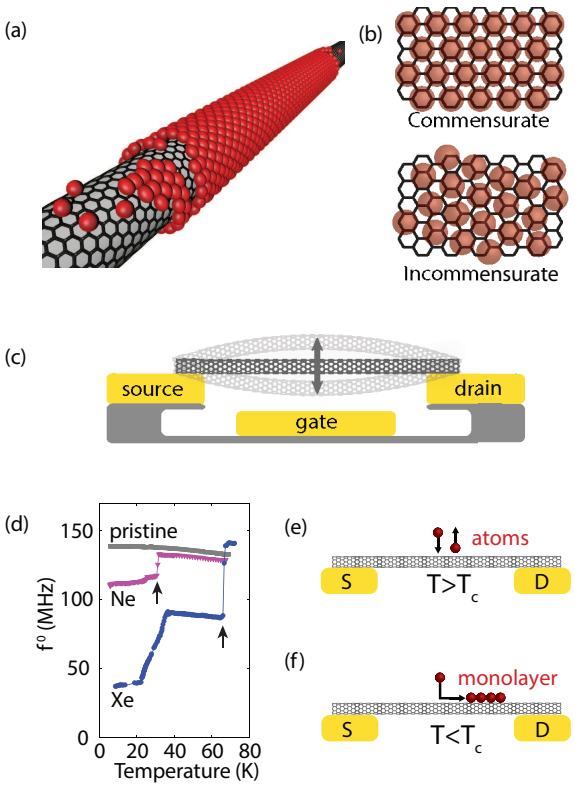

FIG. 1: (a) Growth of an atomic monolayer on a nanotube. (b) Schematics of monolayers in the solid phase that are commensurate (top) and incommensurate (bottom) with the carbon substrate. The adsorbed atoms are represented by red spheres, whereas the carbon surface is depicted by the honeycomb lattice. (c) Layout of the nanotube resonator. (d) Resonance frequency upon lowering temperature while dosing Xe and Ne using a pinhole micromanipulator. The curve labeled "pristine" corresponds to the T dependance of f^0 when we do not dose atoms. The pressure is $3\cdot10^{-7}$ mbar for the Xe and the Ne measurements and $3\cdot10^{-11}$ mbar for the pristine measurement. (e,f) Schematics showing the balance of atoms impinging on and departing from the nanotube above and below the characteristic temperature T_c.

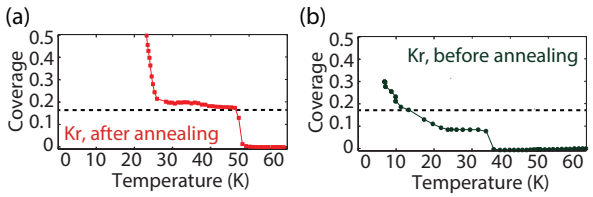

FIG. 2: (a) Coverage upon dosing Kr atoms while lowering the temperature T with a ramping rate 0.016 K/s. (b) Same measurement recorded before having current annealed the nanotube with a T ramping rate 0.033 K/s. The pressure is $3 \cdot 10^{-7}$ mbar for both measurements.

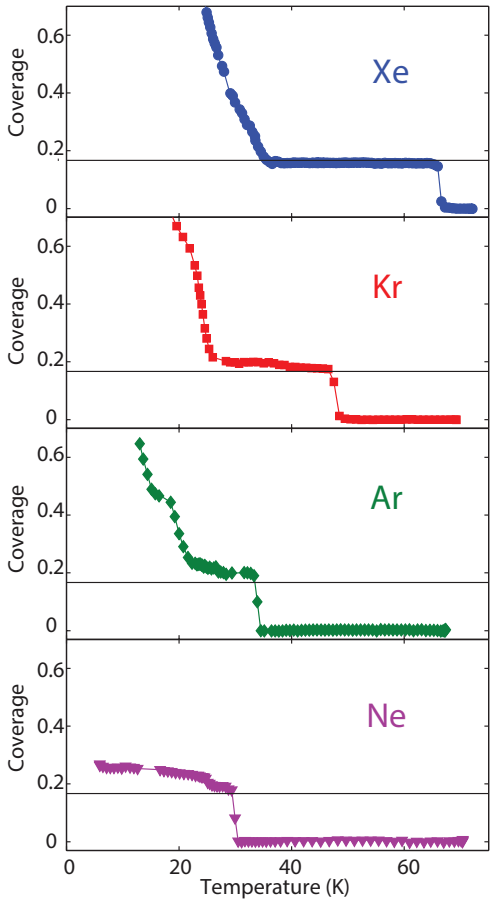

FIG. 3: Coverage upon lowering temperature while dosing Xe, Kr, Ar, and Ne atoms. The pressure is $3 \cdot 10^{-7}$ mbar for all measurements. The T ramping rate is 0.008 K/s for the Xe measurement and 0.016 K/s for the other measurements. The black line corresponds to $\varphi = 1/6$.

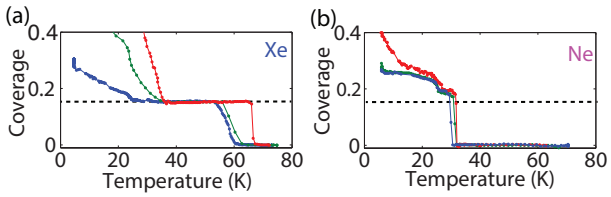

FIG. 4: (a) Coverage upon lowering temperature while dosing Xe atoms. The pressure is $7 \cdot 10^{-8}$, $3 \cdot 10^{-7}$, and $3 \cdot 10^{-7}$ mbar, and the T ramping rate is 0.016, 0.033, and 0.008 K/s for the blue, green, and red lines, respectively. (b) Coverage upon lowering temperature while dosing Ne atoms. The pressure is $3 \cdot 10^{-7}$ mbar for all three measurements, and the T ramping rate is 0.016 K/s for the blue and the green lines and 0.008 K/s for the red line.